Regular Article

IL-7 receptor signaling drives human B-cell progenitor differentiation and expansion.

Supplementary Material

Supplementary Figure Legends

Fig. S1. Flow cytometry plots for in vitro differentiation of human BCP.
(A) Markers used for the definition of the human B-cell progenitor populations in the in vitro experiments. CD34 expression is rapidly downregulated upon in vitro culture and can thus not be used for the identification of BCPs. Markers that are strongly expressed by the given population are depicted in bold, whereas a lack of expression is shown in gray. **(B)** Outcome of $CD34^+$ cell enrichment from CB or BM. Of note, $CD34^+$ enrichment from BM also results in the isolation of BCPs that have already been stimulated with IL-7 in vivo. **(C)** Flow cytometry data of CB cultures at day 14-28 with the gating strategy shown in the top panel. **(D)** Flow cytometry data of BM cultures at day 14.

Fig. S2. Cluster annotation of the scRNA-seq dataset.
(A) Dot plots showing expression of hallmark genes for individual clusters for the combined dataset of controls and patients. **(B)** Representative UMAP plots for selected hallmark genes for the combined dataset of controls and patients, showing the positive cells in the foreground to illustrate their distribution across the different clusters. **(C)** Differences between the proportion of cells in the individual clusters between patients vs. controls as determined by the Single Cell Proportion Test. A permutation test is used to calculate a *P*-value for each cluster and a confidence interval for the magnitude difference via bootstrapping. Shown is a point range plot to display the results.

Fig. S3. Premature expression of cytoplasmic IgM in IL-7Rα-deficient BCPs.
(A-B) Percentage of cytoplasmic IgM-positive CLP (A) and pro-B cells (B) generated from CB-derived hematopoietic progenitors. Flow cytometry plots on the left and quantification of data with dots showing mean and error bars representing the s.e.m. on the right. Statistical analysis was done with a mixed-effects model and corrected for multiple testing according to Šídák. All replicates are shown (n = 7, each with 2-5 replicates). *P*-values are denoted as follows: <0.05 (*), <0.01 (**), <0.001 (***), <0.0001 (****).

Fig. S4. IL-7 signaling has limited effects on apoptosis.
(A) Flow cytometric quantification of apoptotic cells by Annexin V staining of individual BCP populations in BM of controls versus patients, shown for one representative control and one patient. The gray histogram represents a positive control derived from the bimodal Annexin V staining pattern of the entire single cell population of a control sample. **(B)** Flow cytometric quantification of dead cells by Zombie staining of BCP subsets in IL-7 stimulated versus unstimulated CB cultures at day 14. Representative histograms are depicted. Bar graphs show mean with error bars representing the s.e.m. Statistical analysis was performed with multiple unpaired t-tests tests and corrected for multiple comparisons with the Holm-Šídák method (n = 7, each with 2-5 replicates). The gray histogram represents a positive control derived from the bimodal Zombie staining pattern of the entire single cell population of a control sample. **(C)** Flow cytometric quantification of dead cells by Zombie staining of BCP subsets in IL-7 stimulated versus unstimulated BM cultures at day 14. Representative histograms are depicted. Bar graphs show median with error bars representing the IQR. Statistical analysis was performed with

multiple Mann-Whitney tests and corrected for multiple comparisons with the Holm-Šídák method (*n* = 3 BM samples, each with 3-6 replicates). The gray histogram represents a positive control derived from the bimodal Zombie staining pattern of the entire single cell population of a control sample. **(D-E)** GSEA analysis with the apoptosis (D) gene set and p53 signaling (E) gene set performed for the pro-B3 and pro-B4/pre-BI clusters with the differentially expressed genes between patients and controls, showing enrichment of the gene sets in the patients. NS = not significant.

Fig. S5. Expression of selected myeloid markers in scRNA-seq dataset and quantification of myeloid cells in vitro.
(A) Violin plots showing expression of *BACH2*, *EBF1*, and *PAX5* in all clusters in controls and patients. **(B)** Heatmap showing the expression of selected myeloid markers used for figure 4D across all clusters. **(C)** Quantification of myeloid cells defined by the expression of CD33 in CB cultures over the course of the experiment. Bar graphs show median with error bars representing the IQR. Statistical analysis was performed with multiple Mann-Whitney tests and corrected for multiple comparisons with the Holm-Šídák method (*n* = 7, each with 2-5 replicates). **(D)** Violin plot showing expression of *LTB* in all clusters in controls and patients.

Fig. S6. IL-7 signaling enhances EBF1 and PAX5 expression.
(A-B) Flow cytometric quantification of EBF1 (A) and PAX5 (B) expression in individual BCP populations in IL-7 stimulated versus unstimulated BM cultures at day 14. Representative histograms are depicted. Quantification of data is shown in Fig. 5. **(C-D)** Flow cytometric quantification of EBF1 (C) and PAX5 (D) expression in IL-7 stimulated versus unstimulated CB cultures at day 14. Representative histograms are depicted. Bar graphs show mean with error bars representing the s.e.m. Statistical analysis was performed with multiple unpaired t-tests and corrected for multiple comparisons with the Holm-Šídák method (*n* = 7, each with 2-5 replicates). **(E-F)** Flow cytometric quantification of CD79A (E) and CD19 (F) expression in individual BCP populations in IL-7 stimulated versus unstimulated BM cultures at day 14. Representative histograms are depicted. Quantification of data is shown in Fig. 5. *P*-values are denoted as follows: <0.05 (*), <0.01 (**), <0.001 (***), <0.0001 (****).

Fig. S7. Increased expression of JUN and FOS transcription factors in IL-7Rα-deficient BCPs and pediatric BCPs.
(A) Heatmap showing expression of *JUN* and *FOS* family members across all clusters of the scRNA-seq dataset in patients versus controls. **(B)** Heatmap showing expression of *JUN* and *FOS* family members in pediatric and fetal bone marrow pro-B and pre-BI cells. Expression levels are shown as mean signal values. Data taken from Rother et al.[26]

Fig. S8. IL-7Rα deficiency does not have a major effect on N-nucleotide addition but increases *IGH* repertoire clonality.
(A) Flow cytometric quantification of TdT expression in CLP's and pro-B cells in BM of controls versus patients, shown for one representative control and one patient. **(B)** Flow cytometric quantification of TdT-expressing cells in BCP subsets of IL-7 stimulated versus unstimulated BM cultures at day 14. Representative histograms are depicted. Bar graphs show mean with error

bars representing the s.e.m. Statistical analysis was performed with multiple unpaired *t* tests and corrected for multiple comparisons with the Holm-Šídák method (*n* = 3 BM samples, each with 3-6 replicates). **(C)** Junctions of productive and unproductive *IGH* rearrangements of T^- B^+ SCID patients showing N nucleotides, deletions and CDR3 length as indicated (*n* = 3 controls, 3 patients with mutations in the cγ chain, 3 patients with mutations in JAK3, and 2 IL-7Rα-deficient patients). Data shows mean with s.e.m. *P*-values are denoted as follows: <0.05 (*), <0.01 (**), <0.001 (***), <0.0001 (****).

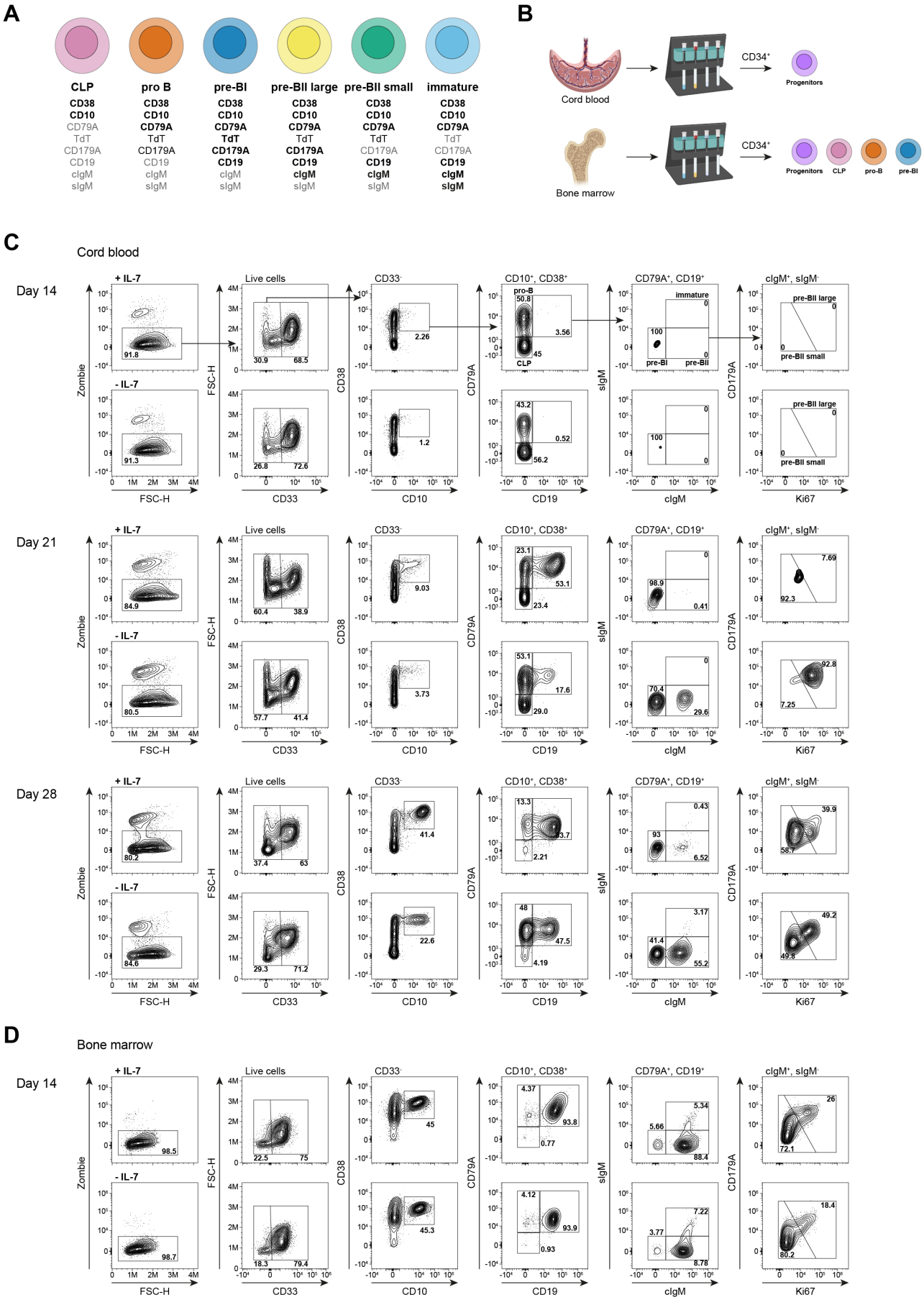

Supplementary Figure 1

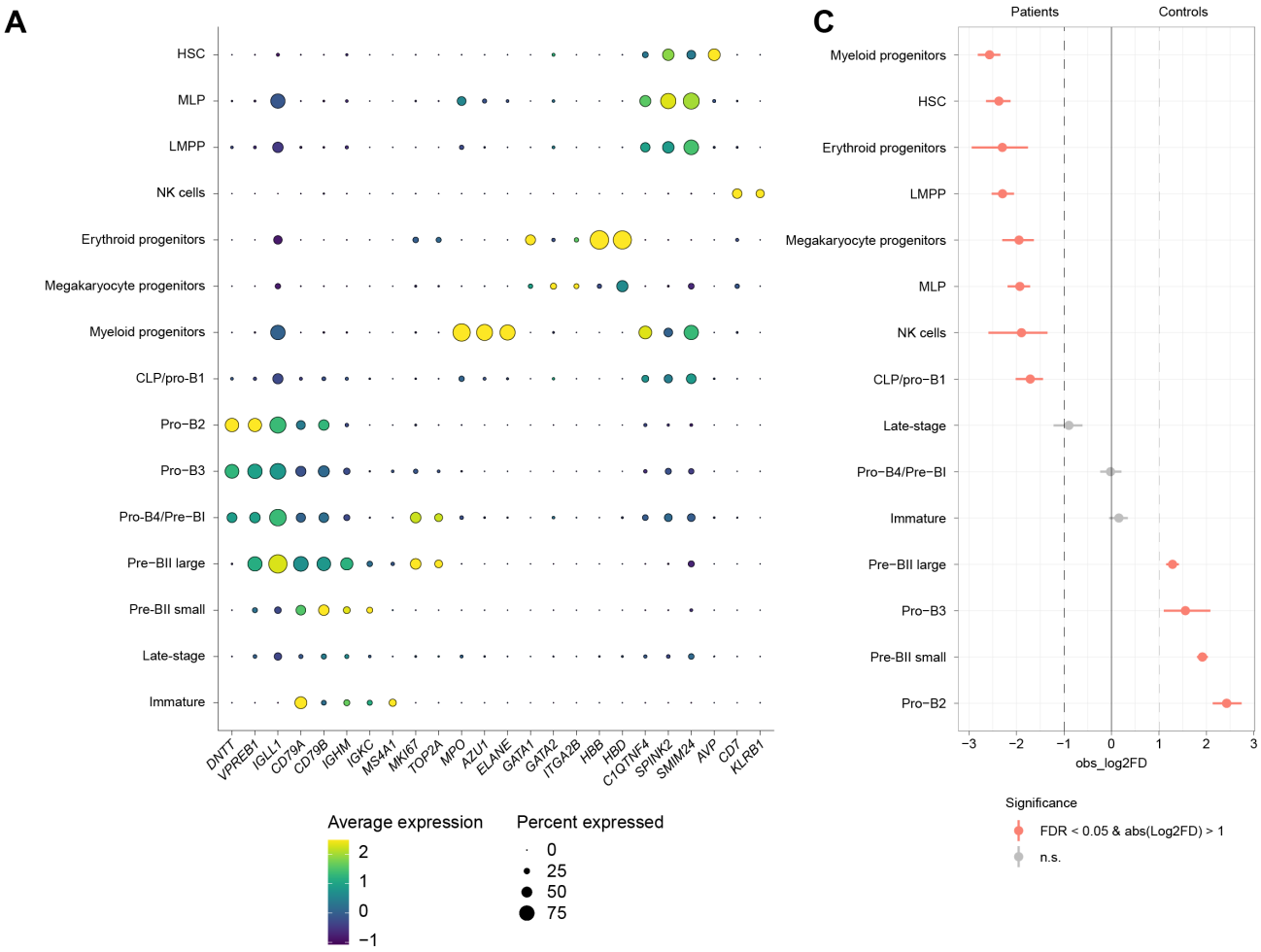

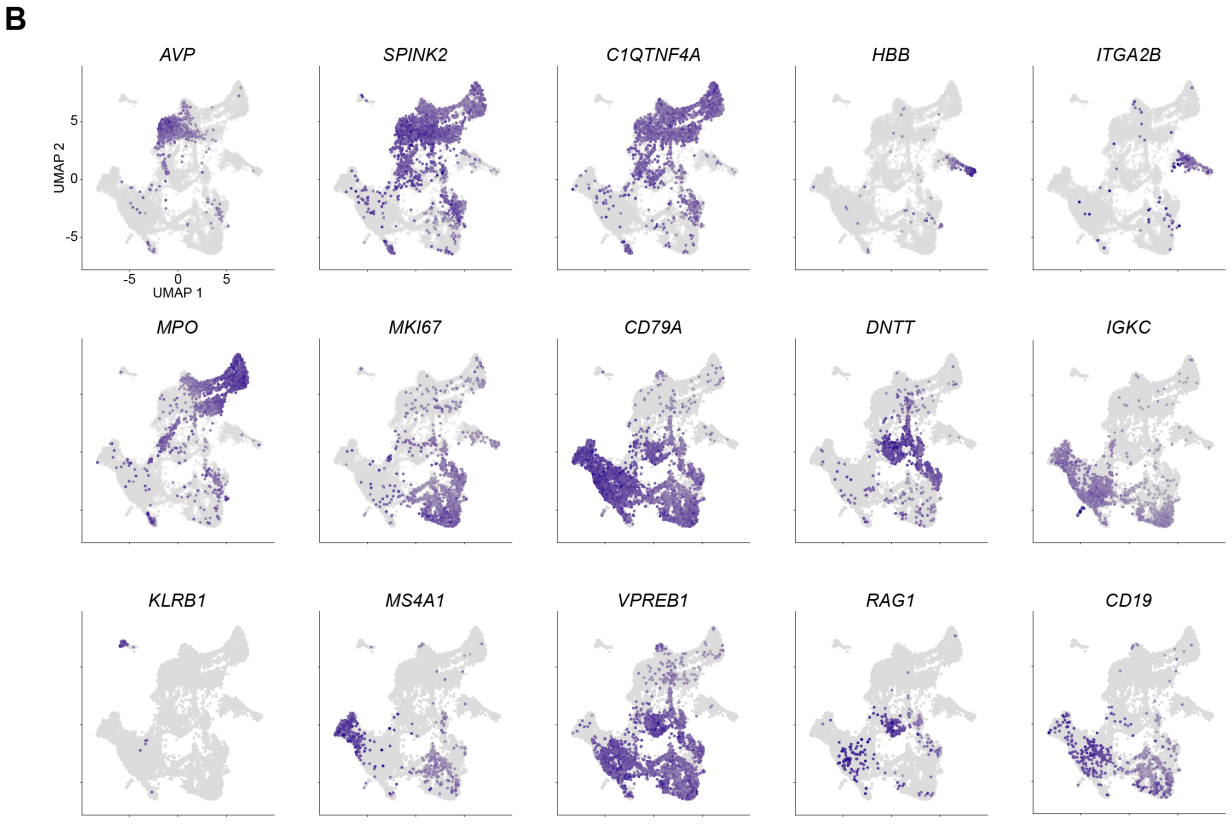

Supplementary Figure 2

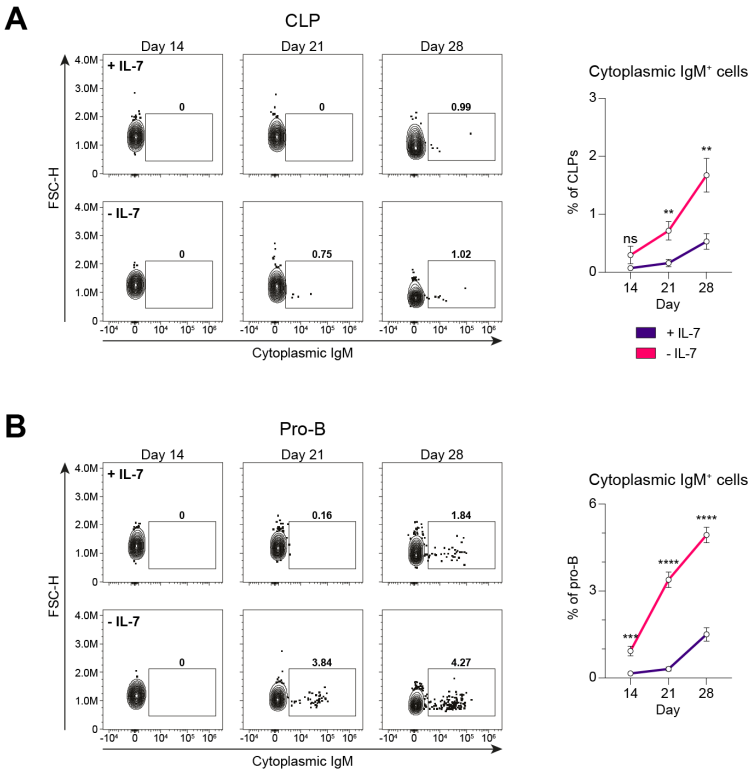

Supplementary Figure 3

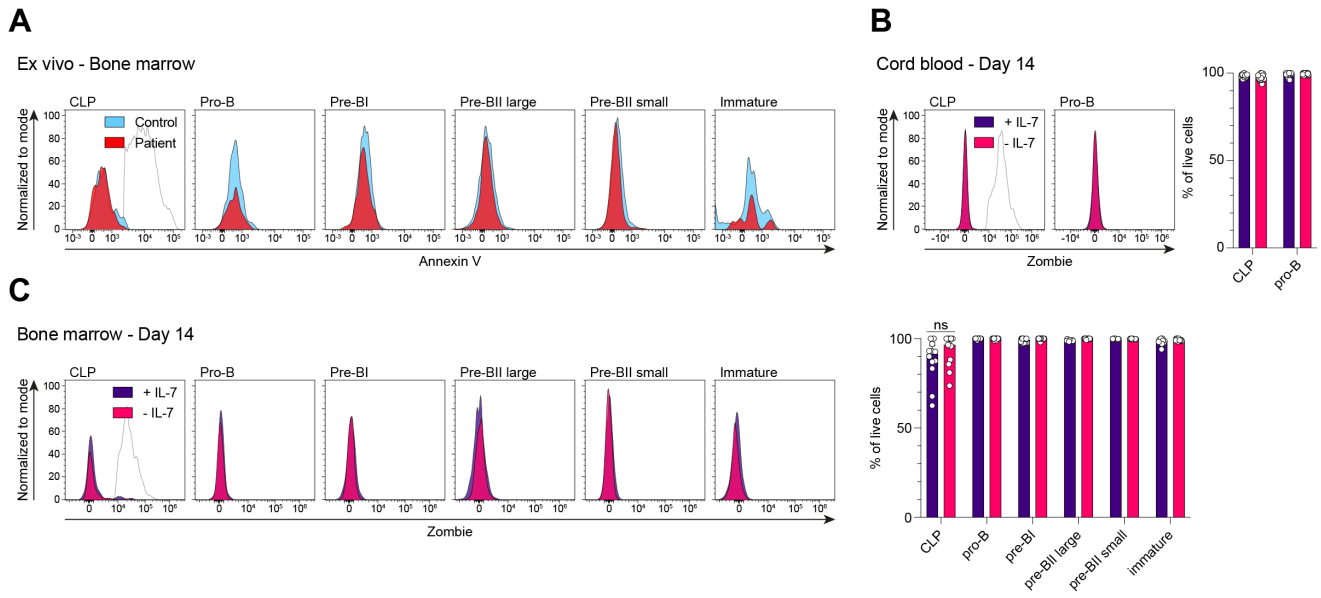

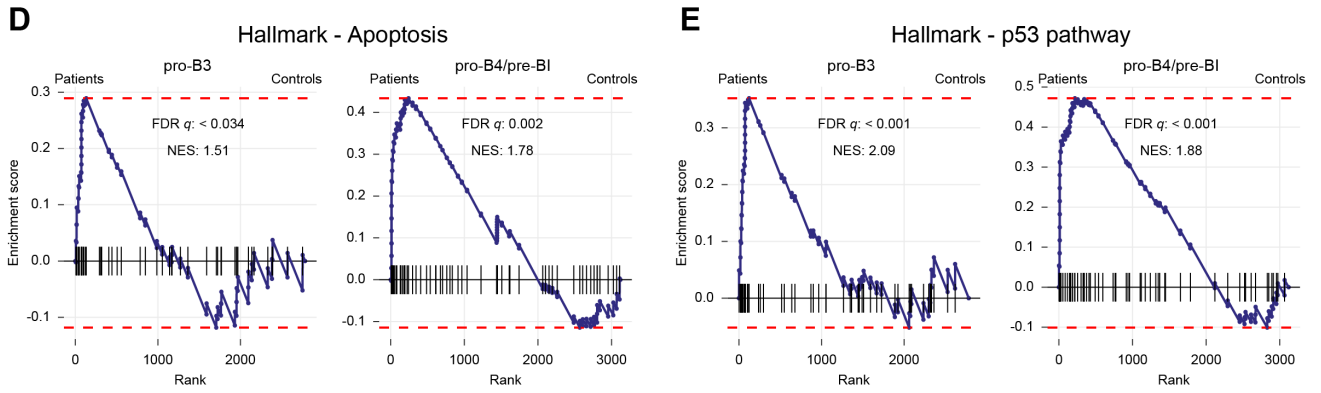

Supplementary Figure 4

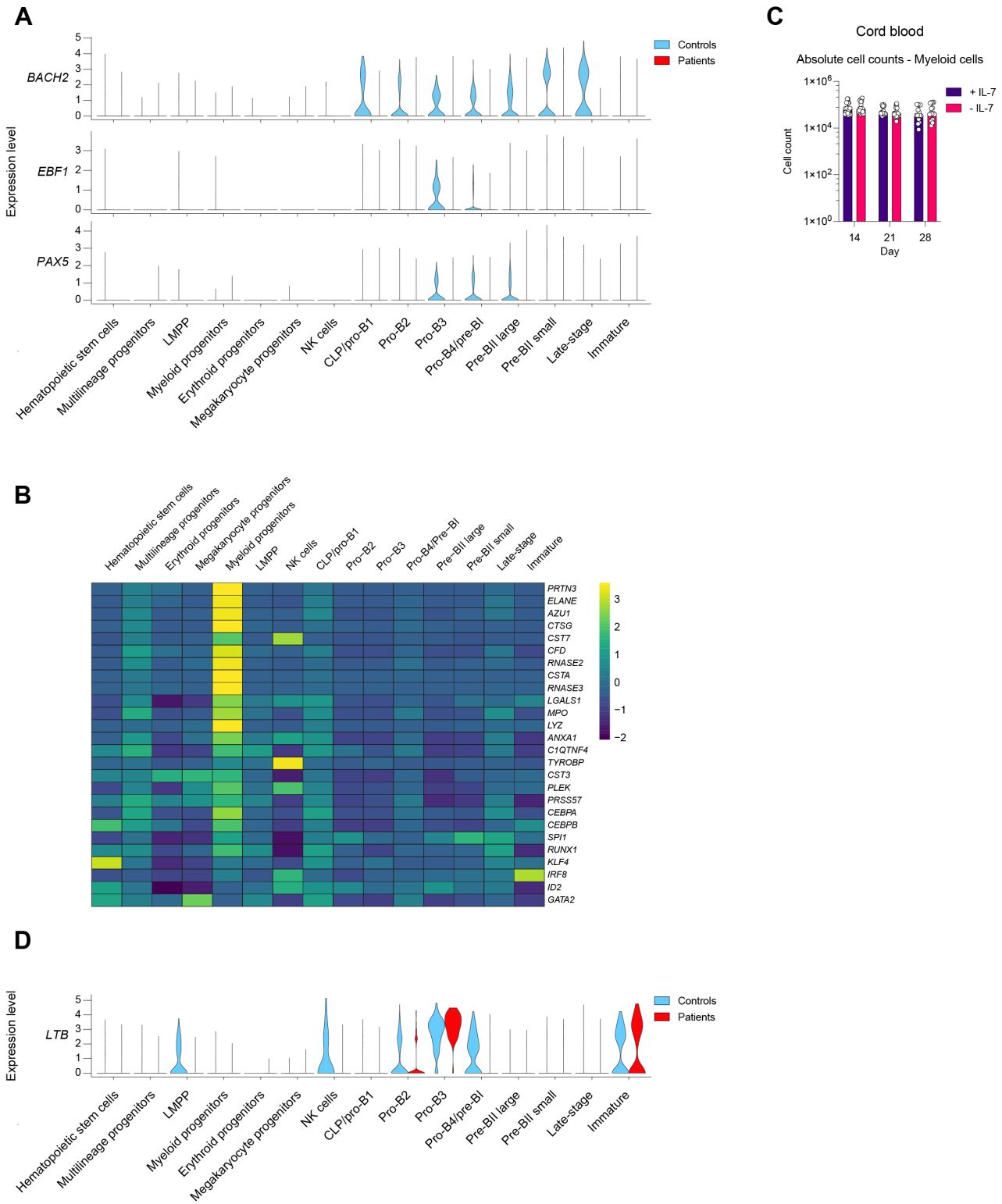

Supplementary Figure 5

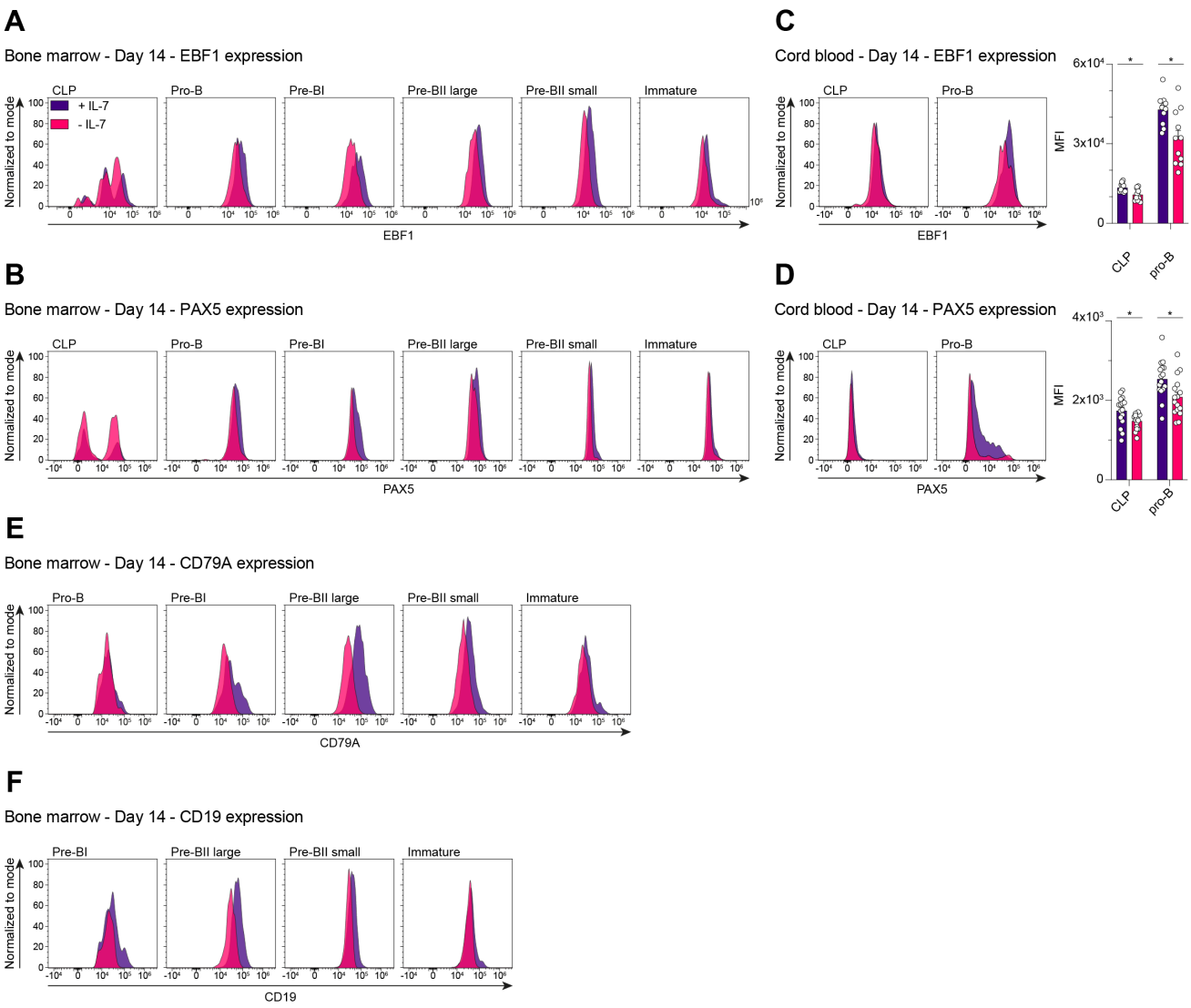

Supplementary Figure 6

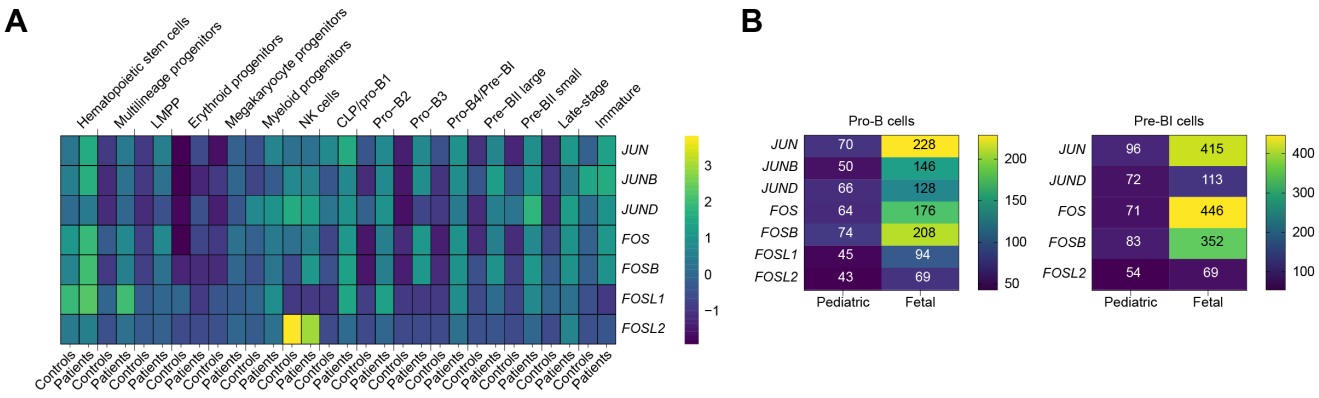

Supplementary Figure 7

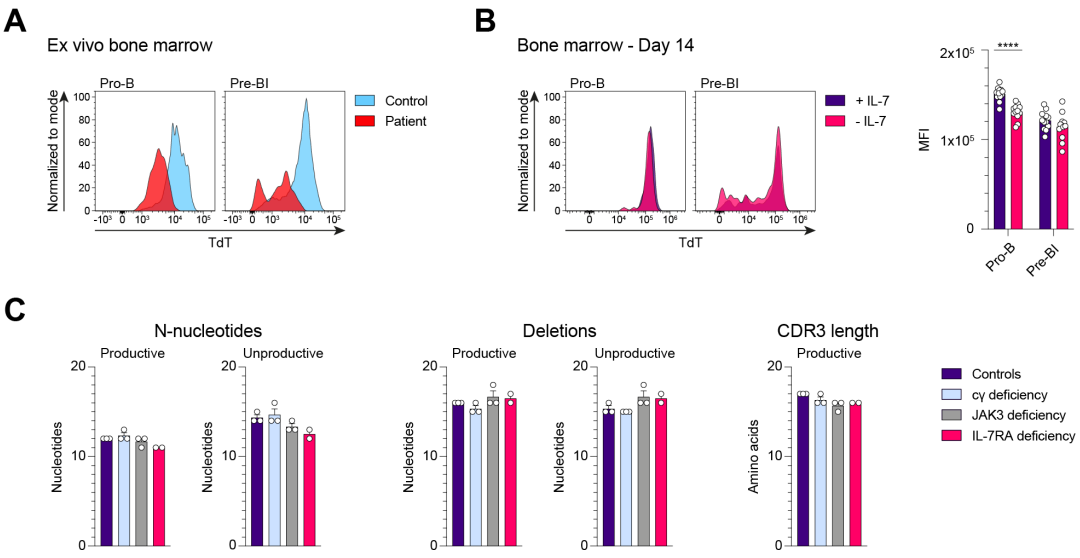

Supplementary Figure 8